Chemosphere 155 (2016) 329–335

Contents lists available at ScienceDirect

Chemosphere

journal homepage: www.elsevier.com/locate/chemosphere

Investigating the environmental factors affecting the toxicity of silver nanoparticles in *Escherichia coli* with dual fluorescence analysis

Wei Hong [a, b], Luzhi Li [a, b], Junting Liang [a, b], Jingjing Wang [a, b], Xuanyu Wang [a, b], Shengmin Xu [a, b], Lijun Wu [a, b], Guoping Zhao [a, b], An Xu [a, b, **], Shaopeng Chen [a, b, *]

[a] Key Laboratory of Ion Beam Bioengineering, Hefei Institutes of Physical Science, China Academy of Sciences, Hefei, Anhui, PR China
[b] Key Laboratory of Environmental Toxicology and Pollution Control Technology of Anhui Province, Hefei, Anhui, PR China

HIGHLIGHTS

- A dual fluorescence flow cytometric analysis for detecting the toxicity of silver nanoparticles was established.
- Cu^{2+} enhanced toxicity of silver nanoparticles but not that of dissolved Ag^{+} ions.
- SDS increased toxicity of silver nanoparticles and dissolved Ag^{+} ions.

GRAPHICAL ABSTRACT

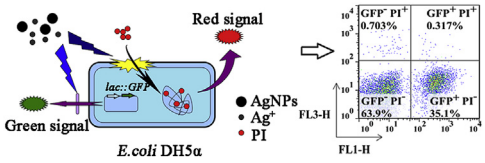

ARTICLE INFO

Article history:
Received 16 January 2016
Received in revised form
31 March 2016
Accepted 20 April 2016
Available online 29 April 2016

Handling Editor: Tamara S. Galloway

Keywords:
Silver nanoparticles
Toxic effects
Dual fluorescence analysis
Environmental factor

ABSTRACT

Flow cytometric investigation of the toxic effects of nanoparticles on bacteria is highly challenging and not sensitive due to the interference of aggregated nanoparticles: aggregated nanoparticles and bacteria are similar in size. In this study, an optimized dual fluorescence flow cytometric analysis was developed using PI-*Lac::GFP* (propidium iodide stained *Escherichia coli* (*lac::GFP*)) to monitor the toxicity of silver nanoparticles (AgNPs). As compared with single fluorescence analysis, the dual fluorescence analysis enabled more accurate evaluation of the toxic effects of AgNPs. We used this dual fluorescence analysis to investigate how AgNPs toxicity was affected by two typical environmental factors, divalent metal ions and surfactants. Our data revealed that Cu^{2+} and SDS significantly enhanced the toxicity of AgNPs in a dose-dependent manner. SDS enhanced the toxicity of both AgNPs and Ag^{+} ions, whereas Cu^{2+} increased the toxicity of AgNPs but not dissolved Ag^{+} ions. Our results suggest that this dual fluorescence analysis can be used to evaluate the toxicity of AgNPs accurately and sensitively.

1. Introduction

Silver nanoparticles (AgNPs) are antibacterial agent that are widely used in consumer products, such as food-packaging films, medicines, cosmetics and textiles (Budama and Çakır, 2013; Abreu et al., 2015). Thus, AgNPs are inevitably released into the environment, for example through washing and aging silver-containing products (Benn and Westerhoff, 2008; Cleveland et al., 2012), and this harms the indigenous microorganisms in an environment and causes potential environmental problems. The interaction of AgNPs with organisms can trigger numerous toxic effects, such as disruption of the cell wall and the cell membrane, inhibition of the activity of several vital enzymes, generation of reactive oxygen species (ROS), induction of DNA damage, and leading to cell death (Li et al., 2009; Marambio-Jones and Hoek, 2010; Prabhu and Poulose, 2012). After AgNPs are released into and accumulated in an aquatic environment, water chemistry strongly impacts the physical and chemical characteristics of the nanoparticles (Sharma et al., 2014; Yin et al., 2015). Consequently, the chemical parameters of water influence AgNPs toxicity and it is crucial to valuate the toxicity of AgNPs after their

* Corresponding author. Hefei Institutes of Physical Science, Chinese Academy of Sciences, PR China.
** Corresponding author. Hefei Institutes of Physical Science, Chinese Academy of Sciences, PR China.
E-mail addresses: anxu@ipp.ac.cn (A. Xu), spchen035@ipp.ac.cn (S. Chen).

http://dx.doi.org/10.1016/j.chemosphere.2016.04.074
0045-6535/

interaction with aqueous liquids. Water chemical parameters, such as high oxidant availability, low pH, high temperature and increased ion length (Liu and Hurt, 2010; Liu et al., 2010) were found to cause a sustained flux of Ag^+ ions from AgNPs, and these factors contributed substantially to AgNPs toxicity (Navarro et al., 2008). Furthermore, several anions (e.g., Cl^-, S^{2-}) (Reinsch et al., 2012; Levard et al., 2013) and organic ligands (e.g., humic acids, cysteine) (Fabrega et al., 2009; Liu et al., 2010) were reported to reduce AgNPs toxicity toward bacteria by the forming a passivating layer on the surface of AgNPs. However, the mechanism of how AgNPs toxicity is affected by divalent metal ions and surfactants remains unknown.

Flow cytometry (FCM) is a powerful tool in toxicology assay (Jung et al., 2008). However, the toxic effects of nanoparticles on bacteria can't be readily detected using FCM because large nanoparticles and aggregated nanoparticles are of a similar size as bacteria, and thus can't be distinguished from bacteria in the forward-scatter/side-scatter (FSC/SSC) plots obtained in FCM. Recently, fluorescent strains with constitutive promoter and reporter gene were used to detect the toxicity of nanoparticles by fluorescence microscopy or fluorescence spectrophotometer. Chattopadhyay's and Gopinath's group reported that the expression of green fluorescent protein (GFP) was reduced in AgNPs treated recombinant *Escherichia coli* (Gogoi et al., 2006; Matai et al., 2014). However, as compared with fluorescence microscopy and fluorescence spectrophotometer, FCM is more efficient and high-throughput, which can provide more details about how the bacteria are affected by AgNPs. Therefore, it is necessary to establish a new flow cytometric method for detecting the toxic effects of nanoparticles on *E. coli*.

To achieve the aforementioned goal, we developed an improved dual fluorescence analysis method involving the use of propidium iodide (PI) and GFP. The GFP fluorescence was used to distinguish living *E. coli* cells from aggregated nanoparticles and dead cells, and PI was used to distinguish dead or compromised cells from living cells and aggregated nanoparticles. AgNPs toxicity was assessed by calculating the ratio of damaged cells to living cells. After optimizing the culture media, exposure time, and analysis methods, we employed the dual fluorescence analysis to evaluate how divalent metal ions and surfactants affected AgNPs toxicity. Our results suggest that this dual fluorescence analysis can be potentially used for assessing the toxic effects of engineered nanomaterials on microorganisms.

2. Materials and methods

2.1. Characterization of AgNPs in test media

AgNPs (10, 40, and 100 nm) were manufactured by Sigma-Aldrich Co. LLC (USA). To compare the sizes, morphology and dissolution of AgNPs in different media, transmission electron microscopy (TEM) measurements and UV–visible absorption spectra were performed. Briefly, 40 nm-AgNPs were suspended in modified Luria-Bertani broth (mLB; LB without NaCl) or 0.2× mLB to a final concentration of 10 μg/mL. The mixtures were incubated at 37 °C under constant shaking (150 rpm). For TEM analysis, samples were incubated for 2 h, and then a 5 μL drop of mixtures was placed on a copper mesh grid with a carbon support film and air-dried, and images were acquired using a high-resolution transmission electron microscope (HRTEM, JEM-2010, Japan). UV–visible spectra were recorded by using a microplate reader (SpectraMax M2, USA) with a wavelength range of 300–600 nm, after incubation of samples for 0, 1, 2, and 4 h.

2.2. Bacterial strain and culture conditions

The bioreporter strain was obtained by transforming pUC18-lac-GFP (a plasmid in which *GFP* is inserted down stream of *lac* promoter) into competent cells (*E. coli* DH5α, *F-φ80d lacZΔM15 Δ(lacZYA-argF) U169 end A1 recA1 hsdR17 (rk-,mk+) supE44λ-thi-1 gyrA96 relA1 phoA*). These *E. coli* DH5α cells carrying pUC18-lac-GFP were used as the source of inocula in experiments. Bacterial cultures were grown in 50 mL of mLB (supplemented with 100 μg/mL ampicillin) for 16 h with agitation (150 rpm) at 37 °C. Then, the bacteria were collected through centrifugation at 10,000 rpm for 3 min and resuspended in growth media.

2.3. Exposure of AgNPs to bioreporter stains

The bioreporter stain (*E. coli* DH5α(*lac::GFP*)) was prepared as described above, resuspended and diluted with 0.2× mLB to approximately 10^6 colony forming units (CFU)/mL. Then, the bacterial cells were exposed to AgNPs (10, 40, and 100 nm) for a designated time at the final concentrations of 0.2, 0.4, and 0.6 μg/mL, respectively. For detecting the effects of divalent metal ions or surfactants on the toxicity of AgNPs, 1 μM divalent metal ions (Ca^{2+}, Cd^{2+}, Cu^{2+}, Fe^{2+}, Mg^{2+}, Mn^{2+}, or Ni^{2+}) or 400 μM surfactants (SDS, Triton X-100, or Tween 20) were added to the bacteria with AgNPs. The concentrations reported here were the final concentrations.

2.4. Colony formating units experiment

For investigating whether growth media affected the antibacterial activity of AgNPs, the traditional toxicological approach of CFU experiment was performed. Briefly, AgNPs preincubated in pure water, 0.2× mLB and mLB for 2 h were added to cells at a final concentration of 2.5 or 5 μg/mL. The mixtures were incubated in 96-well plates (150 μL/well) at 37 °C with shaking (150 rpm) for 2 h, and then 100 μL of the inocula and their 10-fold serial dilutions were plated on LB agar (containing 100 μg/mL ampillin). The CFU was counted after 16 h incubation at 37 °C.

2.5. Flow cytometry analysis

PI is a commonly used fluorescent dye for labeling dead or compromised cells by penetrating the cell membrane and interacting with double-stranded DNA (Spilimbergo et al., 2009). The bioreporter stain (*E. coli* DH5α(*lac::GFP*)) cells treated with AgNPs were washed three times with PBS. PI was added to the suspensions and incubated for 15 min at 4 °C in the dark. Subsequently, the fluorescence of the cells was measured by flow cytometer (BD Calibur, BD biosciences). The BD CellQuest software was used for data acquisition and the FlowJO 7.6.1 software was used for analysis.

The response ratio of fluorescent bacteria to AgNPs exposure was calculated according to the following formula.

$$\text{Response ratio} = \frac{\text{Percentage of GNPP}}{\text{Percentage of GPPN}} \quad \text{(a)}$$

here, GNPP denotes GFP-negative and PI-positive (GFP^-PI^+) bacteria in the upper left quadrant, and GPPN denotes GFP-positive and PI-negative (GFP^+PI^-) bacteria in the lower right quadrant.

To monitor the time-dependent effect of AgNPs, *E. coli* DH5α (*lac::GFP*) cells (10^6 CFU/mL) were treated with 0.4 μg/mL AgNPs (40 nm). After incubation for 30–150 min, the bacteria were washed with PBS, then stained with PI, and analyzed with FCM.

2.6. Statistical analysis

All statistical analysis was performed using the statistical software package OriginPro Version 8.6. All data were presented as

means and standard derivations. The Student's *t*-test was used to assess the significance levels. A P-value of 0.05 or less was considered statistically significant.

3. Results

3.1. Optimization of culture media

The traditional LB medium contains chloride ions and is rich in organic matter which affect the stability of AgNPs. To minimize the influence of exposure media on the physical and chemical properties of AgNPs, nanoparticles were detected by a TEM instrument and a microplate reader after incubation in regular or diluted mLB (LB without sodium chloride). Fig. 1A and C showed that AgNPs with spherical morphology were well dispersal in ddH_2O and 0.2 mLB, while the aggregated nanoparticles were observed in mLB (Fig. 1B). AgNPs had a characteristic UV–visible absorbance spectrum with λ_{max}414 nm. The absorbance of AgNPs in mLB was significantly decreased in a time-dependent manner, but only slightly decreased in 0.2× mLB (Fig. 1D–F). After 2 h incubation, the 414 nm absorbance of AgNPs was 0.51 in ddH_2O, 0.24 in mLB, and 0.44 in 0.2× mLB, respectively. Furthermore, *E. coli* grew stably and proliferated efficiently in 0.2× mLB (Fig. S1A), and the antibacterial activity of AgNPs in 0.2× mLB was not decreased substantially relative to control (Fig. S1B). Based on the results above, 0.2× mLB was used as the basic medium for AgNPs exposure in the following studies.

3.2. Optimization of dual fluorescence analysis

To establish a rapid and accurate method for evaluating the toxicology of nanoparticles by FCM, three analysis strategies were devised and compared as follows: (1) *E. coli* DH5α (*lac::GFP*) cells were exposed to AgNPs and then green fluorescence was analyzed; (2) *E. coli* DH5α cells were exposed to AgNPs and stained with PI, and then red fluorescence of PI was analyzed; (3) *E. coli* DH5α (*lac::GFP*) cells were exposed to AgNPs and stained with PI, and then both GFP fluorescence and PI fluorescence were analyzed (Fig. 2 and Fig. S3). The results obtained using Strategy 1 (Fig. 2A) revealed that, 13.1% and 55.0% of the bacteria lost their green fluorescence (GFP-negative cells, GFP^- cells) in the groups treated with 40 and 100 nm-AgNPs, respectively. This was not consistent with previous studies: smaller sized AgNPs was more toxic than larger sized AgNPs (Sotiriou and Pratsinis, 2010a; Ivask et al., 2014). The aggregated AgNPs were considered as GFP^- cells and the results were not reliable. In the case of Strategy 2, the percentage of PI-positive cells (PI^+ cells) in the control groups (1.72%) was higher than that in group treated with 100 nm-AgNPs (0.938%, Fig. 2B), this was also not reliable because the aggregated AgNPs were counted as living cells (PI^- cells). Lastly, Strategy 3 involved dual fluorescence examination of PI-stained *E. coli* DH5α (*lac::GFP*). As shown in Fig. 2C and Fig. S2C, the influence of aggregated AgNPs was excluded, which were mainly distributed in the area of GFP^-PI^- after flow cytometry dot plot analysis. The Response ratio presenting the toxicity of AgNPs was calculated by the formula (a) which was described in "Material and Methods". The toxicity of AgNPs was accurately exhibited in a size- and concentration-dependent manner (Fig. S3), and these data agreed with the CFU data (data not show) and the results of previous studies (Martínez-Castañón et al., 2008). These findings indicate that the dual fluorescence analysis with PI-stained *E. coli* DH5α (*lac::GFP*) in Strategy 3 could be used in evaluating the toxicity of AgNPs.

3.3. Time response of AgNPs toxicity measured using dual fluorescence analysis

In order to monitor the time response of AgNPs, bacteria were treated with AgNPs for various periods. The response ratio significantly increased with time and peaked at 120 min (Fig. 3). Thus, to obtain the highest response ratio, 120 min was used as

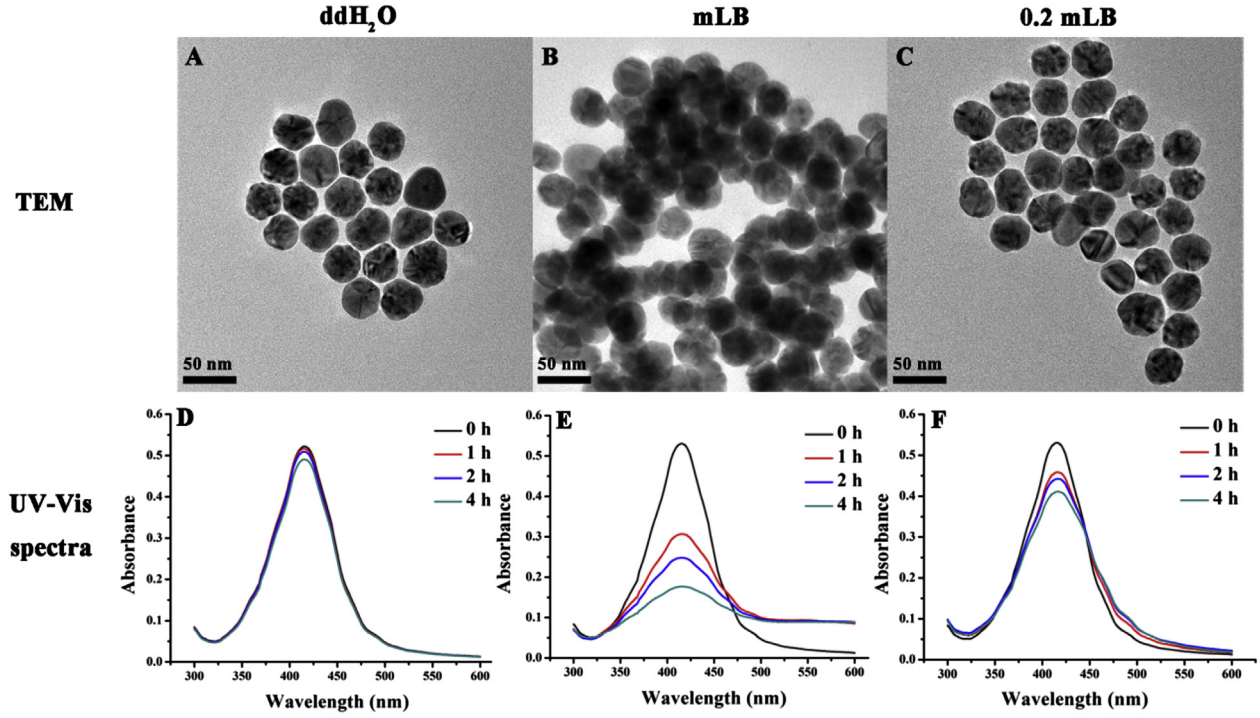

Fig. 1. TEM images (A–C) and UV–vis absorption spectra of 40 nm-AgNPs in different media (D–F). 10 μg/mL 40 nm-AgNPs were preincubated in ddH_2O (A, D), mLB (B, E) and 0.2 mLB (C, F) at 150 rpm and 37 °C. TEM images were recorded after 2 h incubation and UV–vis absorption spectra were recorded at different incubation time.

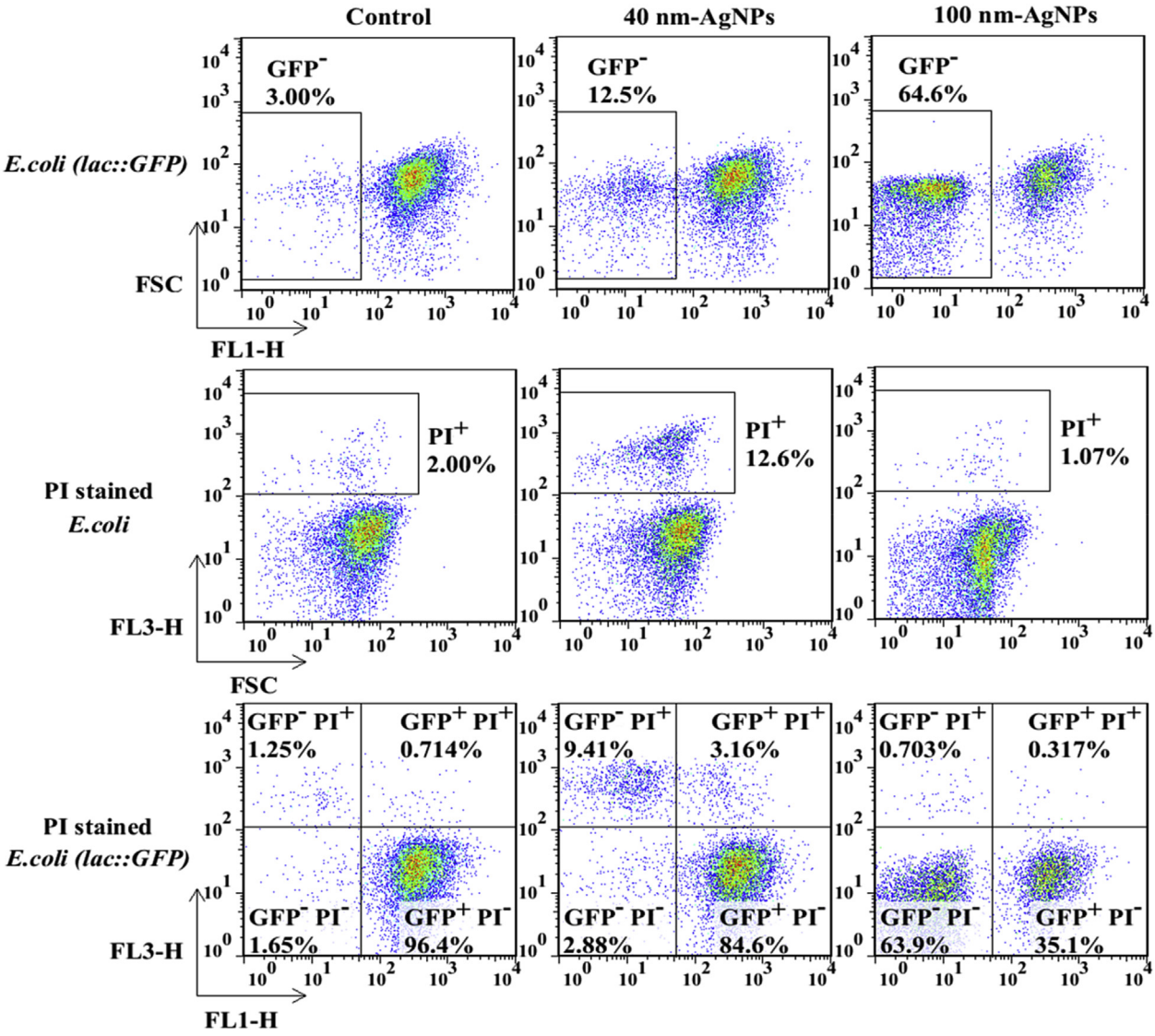

Fig. 2. Flow cytometry dot plot analysis of AgNPs-treated *E. coli*. After exposure to 0.4 μg/mL AgNPs for 2 h, the bacteria were stained with PI and analyzed by FCM: control (left panels), 40 nm-AgNPs (middle panels), and 100 nm-AgNPs (right panels). FSC: forward scattering, FL1-H: green fluorescence due to *lac::GFP*; FL3-H: red fluorescence due to PI.

the measurement time point in the subsequent experiments.

3.4. Effects of divalent metal ions and surfactants on AgNPs toxicity

It's well known that the stability of nanoparticles may be altered in aqueous solution, particularly in the present of certain environmental factors (Choi et al., 2009; Levard et al., 2012). However, very few findings have been reported regarding how divalent metal ions or surfactants influence the toxicology of AgNPs. As shown in Fig. 4A, the response ratio of AgNPs was significantly increased by Cu^{2+} ion (from 4.599 ± 0.162 to 30.500 ± 1.171). Some of divalent ions (Ca^{2+}, Mg^{2+}, Mn^{2+}, Ni^{2+}) exerted no marked effect on the response ratio, and others (Cd^{2+}, Co^{2+}, Fe^{2+}) lowered the response ratio of AgNPs. However, unlike these metal ions, all of the surfactants (SDS, Triton X-100, and Tween 20), could induce the increase of the response ratio. Both Cu^{2+} and SDS enhanced the response ratio of AgNPs in a concentration-dependent manner (Fig. 4C and D). These results suggested that Cu^{2+} and SDS increase toxicity of AgNPs toward *E. coli*.

3.5. Effect of Ag^{+} on AgNPs toxicity after suspension in Cu^{2+} and SDS

Previous studies have demonstrated that the mechanisms of biotoxicity of AgNPs lay in two aspects: particle effects and ion effects (Sotiriou and Pratsinis, 2010b). To investigate the role of dissolved Ag^{+} and that of the particles in the synergistic effects induced by AgNPs and Cu^{2+} (or SDS), *E. coli* cells (*lac::GFP*) were coexposed to Ag^{+} and Cu^{2+} (or SDS). The maximal concentration of dissolved Ag^{+} in 0.2× mLB was 10% as measured by ICP-MS (Wang et al., 2013) (data not shown), so 0.04 μg/mL Ag^{+} ions were used to match the concentration of AgNPs (0.4 μg/mL). Fig. 5 showed that exposure of *E. coli* to either AgNPs and Ag^{+} in 400 μM SDS led to a significant increase in the response ratio (0.22 ± 0.040 with AgNPs, 0.52 ± 0.015 with Ag^{+}) as compared with the control (0.034 ± 0.016). More interestingly, Cu^{2+} enhanced the toxicity of silver nanoparticles (0.62 ± 0.093) but not that of the dissolved Ag^{+} ions (0.171 ± 0.023).

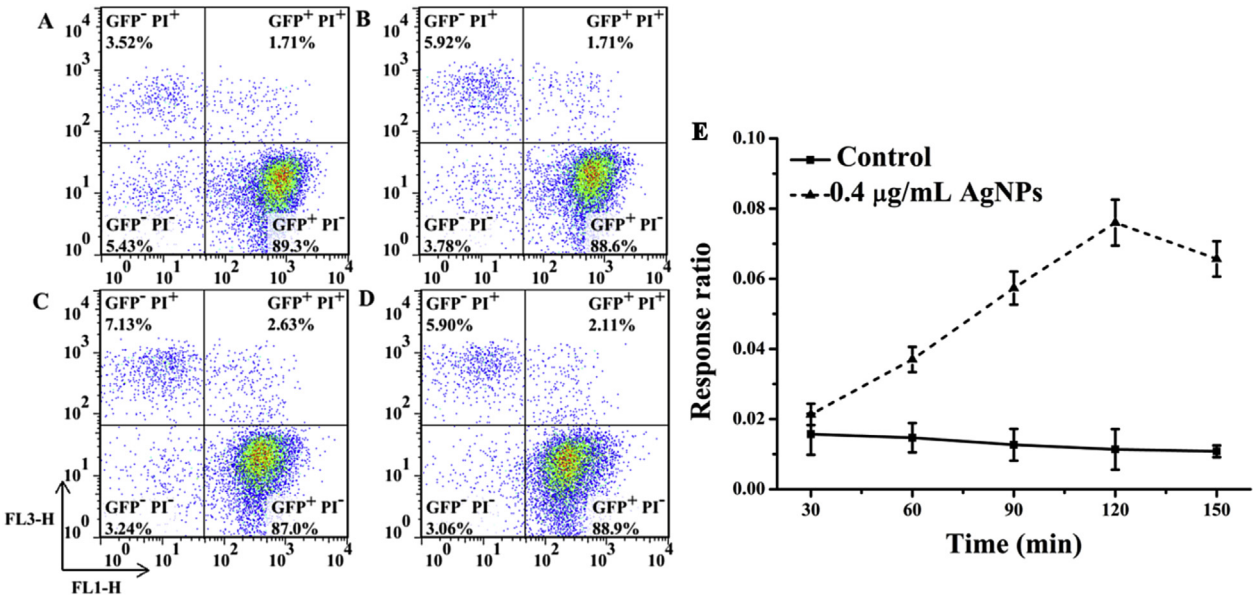

Fig. 3. Dot plot of *E. coli* exposed to 40 nm-AgNPs for: 30 min (A), 60 min (B), 120 min (C), and 150 min (D). (E) Response time-course curves for *E. coli* after incubation with 40 nm-AgNPs. Data are pooled from at least three independent experiments and the results represent mean ± s.d.

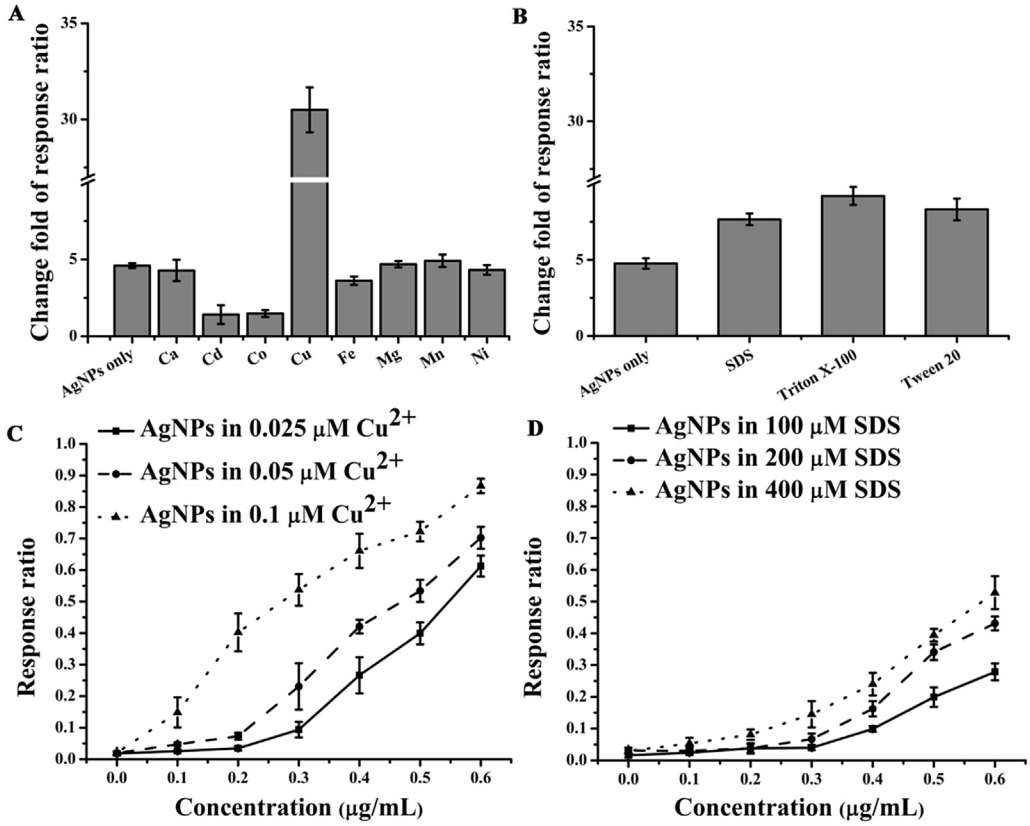

Fig. 4. Effects of divalent metal ions (A) and surfactants (B) on the response ratio and the response ratio after exposure of *E. coli* to 40 nm-AgNPs suspended in solutions containing different concentrations of Cu^{2+} (C) and SDS (D). Data are pooled from at least three independent experiments and the results represent mean ± s.d.

4. Discussion

The ever-increasing use of AgNPs carries with potential eco-toxicological risks (Beddow et al., 2014; Hadrup and Lam, 2014). For a full risk assessment, biomonitoring using bacterial biosensors has come on the scene due to its advantages, such as time-saving, visible responses and low costs (Kumar et al., 2011). In the present study, to monitor the toxicity of AgNPs in aqueous media, a dual fluorescent detection based on *lac::GFP* and PI was developed with an optimized experimental conditions and analysis methods.

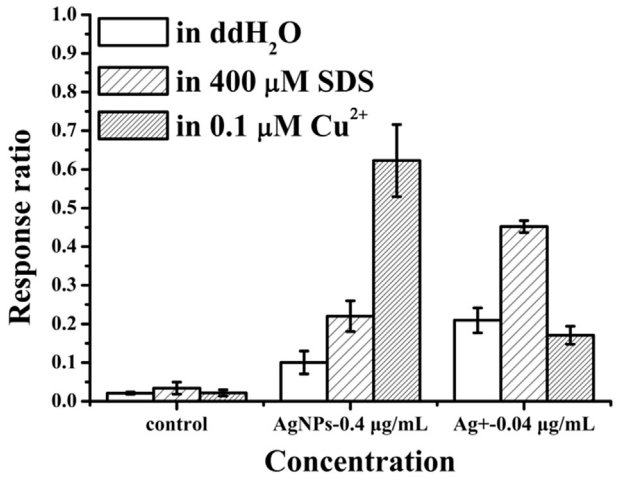

Fig. 5. Comparative study of response ratio between the AgNPs and the Ag^+ ions suspended in 0.1 μM Cu^{2+} or 400 μM SDS. Data are pooled from at least three independent experiments and the results represent mean ± s.d.

AgNPs are highly unstable in LB media. Therefore, LB media are not suitable for analysing the toxicity of AgNPs in most dystrophic environments (e.g., drinking water, river water, and wastewater). If LB media are used to investigate the toxicity of AgNPs to *E. coli*, the stability of AgNPs in media must be considered (Tejamaya et al., 2012). Certain dystrophic media were adopted in recent literature, such as 50 mM sodium *N*-(2-hydroxyethyl) piperazine-*N*′-ethanesulfonic acid (HEPES) buffer (pH 7.0) containing 5 mM glucose (Lok et al., 2006). However, because glucose represses the activity of *lac* promoter (Inada et al., 1996), these media couldn't be used here. The test medium in this study was optimized based on modified-LB medium (LB lacking NaCl, which can potentially cause AgNPs dissolution and aggregation) (Levard et al., 2013). During the incubation time in 0.2× mLB, *E. coli* grew and proliferated efficiently, and AgNPs effectively maintained their size and morphology (Fig. S1).

Wang et al. reported that AgNPs suppressed the transcription of genes involved in the carbon and energy metabolism (*lacA* and *ndh*) (Wang et al., 2013). In this study, *E. coli* cells harboring a plasmid constitutively expressed *GFP* under the control of *lac* promoter (*lac::GFP*) were used as the biosensor strains. This biosensor system can respond to the inhibition of growth and metabolism during the exposure to toxicants. Fig. S2 revealed that the expression of *GFP* was closely related to the growth rate of *E. coli*, even under AgNPs exposure, indicating that the fluorescence of *E. coli* (*lac::GFP*) is a suitable indicator of cell growth.

High-throughput flow cytometry is a powerful tool for toxicological research (Hewitt et al., 2001; Liang et al., 2014). However, the toxicity of nanoparticles cannot be readily measured using FCM due to the interference caused by aggregated nanoparticles (Römer et al., 2011; Li and Lenhart, 2012). Two strategies have been used to solve this problem. In one approach, fluorescent nanoparticles—quantum dots or fluorescein-labeled nanoparticles—are used to distinguish *E. coli* cells and aggregated nanoparticles (Ibanez-Peral et al., 2008; Si et al., 2015). Unfortunately, the fluorescein and quantum dot can increase the extra burden of cells, and trigger more complex physiological response. Another approach involves using fluorescent dyes or proteins to label *E. coli* cells. PI and SYTO9 are two dyes used commonly in flow cytometric analysis of bacterial viability (Stiefel et al., 2015). However, the populations of living, compromised, and dead cells were not markedly distincted from each other with PI-SYTO9 dual staining in FCM plots (Lehtinen et al., 2004). In the present study, dual fluorescent detection with PI-*lac::GFP* assay was used to detect the toxicity of AgNPs, and successfully distinguished the dead or compromised bacteria from living bacteria and aggregated nanoparticles. As shown in Fig. 2C, populations of living cells, compromised cells, dead cells, and aggregated AgNPs were clearly separated into 4 quadrant gates, respectively. The interference of aggregated AgNPs was excluded effectively, which improved the accuracy and sensitivity of the toxicity analysis with FCM. Furthermore, the sensitivity of the toxicity analysis was improved here by optimizing the calculation of the response ratio, the components of culture media, and the exposure time. Moreover, as described above, *lac::GFP* was used not only to differentiate between the bacteria and aggregated nanoparticles, but also to obtain detailed information regarding the toxic effect of AgNPs on cell growth and energy metabolism through comparison of fluorescence intensities.

The interaction of released AgNPs with environmental factors is unavoidable. Ionic composition, ionic strength, pH, organic matter, persistent toxic substances, and surfactants all affect the transport and transformation of AgNPs, and this ultimately results in the differences observed in bioavailability and toxicity of AgNPs. In the present study, with dual fluorescence detection, the influence of divalent metal ions and surfactants on the toxicity of AgNPs was analyzed by high-throughput FCM. Cu^{2+} is a typical toxic divalent metal ion that is widely present in the environment, and SDS is a frequently detected surfactant in water bodies. However, very few studies to date have investigated whether Cu^{2+} and SDS affect AgNPs toxicity. Our work revealed that Cu^{2+} and SDS increased AgNPs toxicity toward *E. coli*. Intriguingly, Cu^{2+} enhanced the toxicity of AgNPs but not dissolved Ag^+, whereas SDS increased the toxicity of both AgNPs and Ag^+, which implies that the toxicity mechanisms involved here are different. These results suggest that the effects of factors present in aquatic environments must be considered during the toxicity analysis of AgNPs.

Acknowledgements

This work was supported in part by grants from Major National Scientific Research Projects, 2014CB932002; Strategic Leading Science & Technology Program (B), XDB14030502; The Major/Innovative Program of Development Foundation of Hefei Center for Physical Science and Technology, 2014FXCX010; CASHIPS director's fund, YZJJ201501; The CAS/SAFEA International Partnership Program for Creative Research Teams.

Appendix A. Supplementary data

Supplementary data related to this article can be found at http://dx.doi.org/10.1016/j.chemosphere.2016.04.074.

References

Abreu, A.S., Oliveira, M., de Sá, A., Rodrigues, R.M., Cerqueira, M.A., Vicente, A.A., Machado, A.V., 2015. Antimicrobial nanostructured starch based films for packaging. Carbohydr. Polym. 129, 127–134.
Beddow, J., Stolpe, B., Cole, P., Lead, J.R., Sapp, M., Lyons, B.P., Colbeck, I., Whitby, C., 2014. Effects of engineered silver nanoparticles on the growth and activity of ecologically important microbes. Environ. Microbiol. Rep. 6, 448–458.
Benn, T.M., Westerhoff, P., 2008. Nanoparticle silver released into water from commercially available sock fabrics. Environ. Sci. Technol. 42, 4133–4139.
Budama, L., Çakır, B.A., Topel, Ö., Hoda, N., 2013. A new strategy for producing antibacterial textile surfaces using silver nanoparticles. Chem. Eng. J. 228, 489–495.
Choi, O., Clevenger, T.E., Deng, B., Surampalli, R.Y., Ross Jr., L., Hu, Z., 2009. Role of sulfide and ligand strength in controlling nanosilver toxicity. Water Res. 43, 1879–1886.
Cleveland, D., Long, S.E., Pennington, P.L., Cooper, E., Fulton, M.H., Scott, G.I., Brewer, T., Davis, J., Petersen, E.J., Wood, L., 2012. Pilot estuarine mesocosm study on the environmental fate of Silver nanomaterials leached from

consumer products. Sci. Total Environ. 421–422, 267–272.
Fabrega, J., Fawcett, S.R., Renshaw, J.C., Lead, J.R., 2009. Silver nanoparticle impact on bacterial growth: effect of pH, concentration, and organic matter. Environ. Sci. Technol. 43, 7285–7290.
Gogoi, S.K., Gopinath, P., Paul, A., Ramesh, A., Ghosh, S.S., Chattopadhyay, A., 2006. Green fluorescent protein-expressing Escherichia coli as a model system for investigating the antimicrobial activities of silver nanoparticles. Langmuir 22, 9322–9328.
Hadrup, N., Lam, H.R., 2014. Oral toxicity of silver ions, silver nanoparticles and colloidal silver–a review. Regul. Toxicol. Pharmacol. 68, 1–7.
Hewitt, C., Bellara, S., Andreani, A., Nebe-von-Caron, G., McFarlane, C., 2001. An evaluation of the anti-bacterial action of ceramic powder slurries using multi-parameter flow cytometry. Biotechnol. Lett. 23, 667–675.
Ibanez-Peral, R., Bergquist, P.L., Walter, M.R., Gibbs, M., Goldys, E.M., Ferrari, B., 2008. Potential use of quantum dots in flow cytometry. Int. J. Mol. Sci. 9, 2622–2638.
Inada, T., Kimata, K., Aiba, H., 1996. Mechanism responsible for glucose-lactose diauxie in Escherichia coli: challenge to the cAMP model. Genes Cells 1, 293–301.
Ivask, A., Kurvet, I., Kasemets, K., Blinova, I., Aruoja, V., Suppi, S., Vija, H., Kakinen, A., Titma, T., Heinlaan, M., Visnapuu, M., Koller, D., Kisand, V., Kahru, A., 2014. Size-dependent toxicity of silver nanoparticles to bacteria, yeast, algae, crustaceans and mammalian cells in vitro. PLoS One 9.
Jung, W.K., Koo, H.C., Kim, K.W., Shin, S., Kim, S.H., Park, Y.H., 2008. Antibacterial activity and mechanism of action of the silver ion in Staphylococcus aureus and Escherichia coli. Appl. Environ. Microbiol. 74, 2171–2178.
Kumar, A., Pandey, A.K., Singh, S.S., Shanker, R., Dhawan, A., 2011. A flow cytometric method to assess nanoparticle uptake in bacteria. Cytom. A 79, 707–712.
Lehtinen, J., Nuutila, J., Lilius, E.M., 2004. Green fluorescent protein-propidium iodide (GFP-PI) based assay for flow cytometric measurement of bacterial viability. Cytom. A 60, 165–172.
Levard, C., Hotze, E.M., Lowry, G.V., Brown Jr., G.E., 2012. Environmental transformations of silver nanoparticles: impact on stability and toxicity. Environ. Sci. Technol. 46, 6900–6914.
Levard, C., Mitra, S., Yang, T., Jew, A.D., Badireddy, A.R., Lowry, G.V., Brown Jr., G.E., 2013. Effect of chloride on the dissolution rate of silver nanoparticles and toxicity to E. coli. Environ. Sci. Technol. 47, 5738–5745.
Li, W.-R., Xie, X.-B., Shi, Q.-S., Zeng, H.-Y., OU-Yang, Y.-S., Chen, Y.-B., 2009. Antibacterial activity and mechanism of silver nanoparticles on Escherichia coli. Appl. Microbiol. Biotechnol. 85, 1115–1122.
Li, X., Lenhart, J.J., 2012. Aggregation and dissolution of silver nanoparticles in natural surface water. Environ. Sci. Technol. 46, 5378–5386.
Liang, X., Soupir, M.L., Rigby, S., Jarboe, L.R., Zhang, W., 2014. Flow cytometry is a promising and rapid method for differentiating between freely suspended Escherichia coli and E. coli attached to clay particles. J. Appl. Microbiol. 117, 1730–1739.
Liu, J., Hurt, R.H., 2010. Ion release kinetics and particle persistence in aqueous nano-silver colloids. Environ. Sci. Technol. 44, 2169–2175.
Liu, J., Sonshine, D.A., Shervani, S., Hurt, R.H., 2010. Controlled release of biologically active silver from nanosilver surfaces. ACS Nano 4, 6903–6913.
Lok, C.N., Ho, C.M., Chen, R., He, Q.Y., Yu, W.Y., Sun, H., Tam, P.K., Chiu, J.F., Che, C.M., 2006. Proteomic analysis of the mode of antibacterial action of silver nanoparticles. J. Proteome Res. 5, 916–924.
Marambio-Jones, C., Hoek, E.M.V., 2010. A review of the antibacterial effects of silver nanomaterials and potential implications for human health and the environment. J. Nanoparticle Res. 12, 1531–1551.
Martínez-Castañón, G.A., Niño-Martínez, N., Martínez-Gutierrez, F., Martínez-Mendoza, J.R., Ruiz, F., 2008. Synthesis and antibacterial activity of silver nanoparticles with different sizes. J. Nanoparticle Res. 10, 1343–1348.
Matai, I., Sachdev, A., Dubey, P., Kumar, S.U., Bhushan, B., Gopinath, P., 2014. Antibacterial activity and mechanism of Ag-ZnO nanocomposite on S. aureus and GFP-expressing antibiotic resistant E. coli. Colloids Surf. B Biointerfaces 115, 359–367.
Navarro, E., Piccapietra, F., Wagner, B., Marconi, F., Kaegi, R., Odzak, N., Sigg, L., Behra, R., 2008. Toxicity of silver nanoparticles to Chlamydomonas reinhardtii. Environ. Sci. Technol. 42, 8959–8964.
Prabhu, S., Poulose, E.K., 2012. Silver nanoparticles: mechanism of antimicrobial action, synthesis, medical applications, and toxicity effects. Int. Nano Lett. 2, 1–10.
Römer, I., White, T.A., Baalousha, M., Chipman, K., Viant, M.R., Lead, J.R., 2011. Aggregation and dispersion of silver nanoparticles in exposure media for aquatic toxicity tests. J. Chromatogr. A 1218, 4226–4233.
Reinsch, B.C., Levard, C., Li, Z., Ma, R., Wise, A., Gregory, K.B., Brown Jr., G.E., Lowry, G.V., 2012. Sulfidation of silver nanoparticles decreases Escherichia coli growth inhibition. Environ. Sci. Technol. 46, 6992–7000.
Sharma, V.K., Siskova, K.M., Zboril, R., Gardea-Torresdey, J.L., 2014. Organic-coated silver nanoparticles in biological and environmental conditions: fate, stability and toxicity. Adv. Colloid Interface Sci. 204, 15–34.
Si, Y., Grazon, C., Clavier, G., Rieger, J., Audibert, J.F., Sclavi, B., Meallet-Renault, R., 2015. Rapid and accurate detection of Escherichia coli growth by fluorescent pH-sensitive organic nanoparticles for high-throughput screening applications. Biosens. Bioelectron. 75, 320–327.
Sotiriou, G.A., Pratsinis, S.E., 2010a. Antibacterial activity of nanosilver ions and particles. Environ. Sci. Technol. 44, 5649–5654.
Sotiriou, G.A., Pratsinis, S.E., 2010b. Antibacterial activity of nanosilver ions and particles. Environ. Sci. Technol. 44, 5649–5654.
Spilimbergo, S., Mantoan, D., Quaranta, A., Mea, G.D., 2009. Real-time monitoring of cell membrane modification during supercritical CO2 pasteurization. J. Supercrit. Fluids 48, 93–97.
Stiefel, P., Schmidt-Emrich, S., Maniura-Weber, K., Ren, Q., 2015. Critical aspects of using bacterial cell viability assays with the fluorophores SYTO9 and propidium iodide. BMC Microbiol. 15, 0315–0376.
Tejamaya, M., Romer, I., Merrifield, R.C., Lead, J.R., 2012. Stability of citrate, PVP, and PEG coated silver nanoparticles in ecotoxicology media. Environ. Sci. Technol. 46, 7011–7017.
Wang, Z., Liu, S., Ma, J., Qu, G., Wang, X., Yu, S., He, J., Liu, J., Xia, T., Jiang, G.B., 2013. Silver nanoparticles induced RNA polymerase-silver binding and RNA transcription inhibition in erythroid progenitor cells. ACS Nano 7, 4171–4186.
Yin, Y., Yang, X., Zhou, X., Wang, W., Yu, S., Liu, J., Jiang, G., 2015. Water chemistry controlled aggregation and photo-transformation of silver nanoparticles in environmental waters. J. Environ. Sci. 34, 116–125.